

Oil-Film Interferometry Measurements

Data Acquisition and Procedures

Skin friction measurements on both the boundary layer development plate, and start and downstream end of the ramp were acquired via the oil-film interferometry (OFI) technique. This technique relates the skin friction to the thickness of a sheared film of oil which, in turn, is related to the distance between optical interference fringes produced by monochromatic light reflecting from both the bottom and top of the film. Clearco silicon oils with nominal viscosities of 1,000 and 200 cSt were used as the shearing fluids. Their corresponding specific gravities were 0.974 and 0.969 with refractive indices of 1.4031 and 1.4026, respectively, for the 1,000 and 200 cSt oils. Since aluminum produces inherently poor fringe patterns, the oil was applied to a layer of 5 mil Kapton, placed over the polished aluminum surface. This method produced adequate optical fringe patterns. Adjacent to the Kapton film, a small thin stainless-steel ruler was secured to the surface to serve as a fiduciary marker for measuring the fringe spacing. The ruler was located along the tunnel centerline and the Kapton to either side of it. This ensured that all measurements were collected in the uniform flow region.

In the skin friction measurements, the wind tunnel was run for 20, 30, 40, or 50 minutes and the freestream temperature and dynamic pressure were recorded at 10 Hz over the entire length of the run including startup and shut down. The temperature was recorded using a K-type thermocouple protruding through the -Z wall and located at $X = -0.91$ m and $Y = 0.42$ m. The dynamic pressure was recorded using a pitot-static tube located at $X = -0.87$ m, $Y = 0.52$ m, and $Z = -0.19$ m and connected to the Scanivalve SSS-48C pneumatic scanner discussed previously.

To acquire the interferogram images, the test fixture, shown in Figure 1, was constructed that allowed both the camera and monochromatic light source to be fixed with respect to each other and quickly positioned in the wind tunnel after the test. A sodium lamp with wavelength of 589 nm was used as the monochromatic light source and images were acquired using a Canon Rebel t6 camera featuring a resolution of 5184 x 3456 pixels. The camera was focused and triggered remotely via a computer desktop application. Multiple images were acquired during each run and multiple runs, with differing run times, were conducted for each location of interest.



Figure 1 Photograph of test fixture, shown in place at the $X = -0.678$ m location, developed to illuminate and photograph the interferogram images.

Processing of Data

The resulting interferogram images were then analyzed in MATLAB to determine the fringe spacing which was defined as distance between successive minima or maxima in light intensity. A summary of this process is as follows. First the images were loaded into MATLAB and two points on the ruler were selected in terms of their pixel locations. This pixel distance was then converted to physical distance using an L2-norm and the known distance on the ruler. Next a subregion of the image was selected as the interrogation region to determine the fringe spacing. This region was divided into pixel wide streamwise slices over which each region was fit with two different order Fourier series ranging from 2nd order to 8th order. The mean of the fit was removed and the distance between each minimum value was calculated and converted to physical distance. These distances were then filtered to remove outliers and partial fringes and the mean of the remaining values was taken.

This process was repeated over the entire span of the interrogation region and the distances were averaged for both order Fourier series. If the difference in the final mean fringe spacing between the two different fits was substantial, the filtering criteria was adjusted, or the interrogation region modified until a satisfactory agreement was reached. The fringe spacing value used for each run was the average of the two Fourier series fits. Figure 2 shows an example interferogram image with the ruler and interrogation regions highlighted. The flow is from top to bottom with the start of the ramp, $X = 0$ m, occurring at the 2 in mark on the ruler, hence this location is designated as $X = 0.007$ m. Once processed, the fringe spacing was calculated to be $\Delta x = 3.542$ mm and $\Delta x = 3.560$ mm for 7th and 2nd order Fourier series respectively. Figure 3 shows the histograms and sample Fourier series fits for this interrogation region.

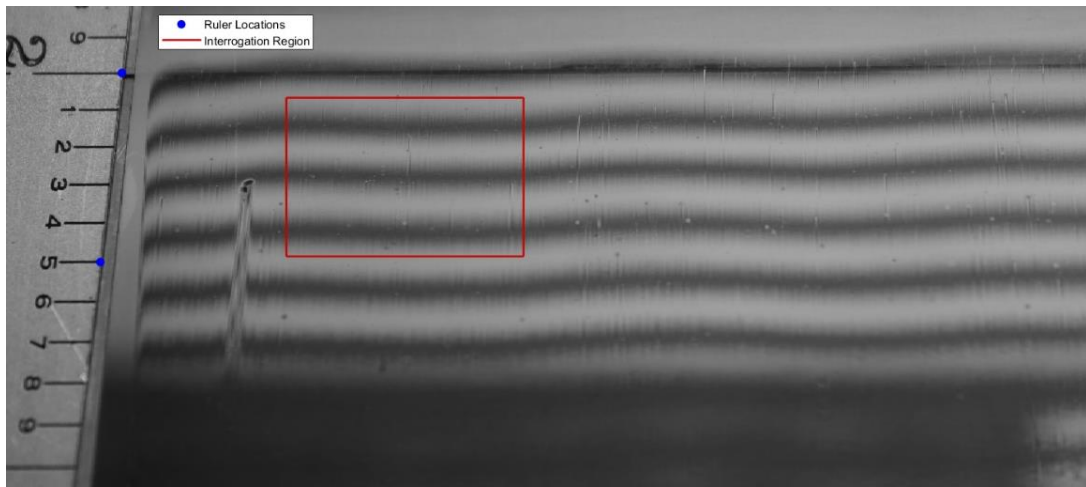


Figure 2 Interferogram example for Case B taken at $X = 0.007$ m and yielding a fringe spacing of $\Delta x = 3.55$ mm and skin friction coefficient of $C_f = 0.00272$.

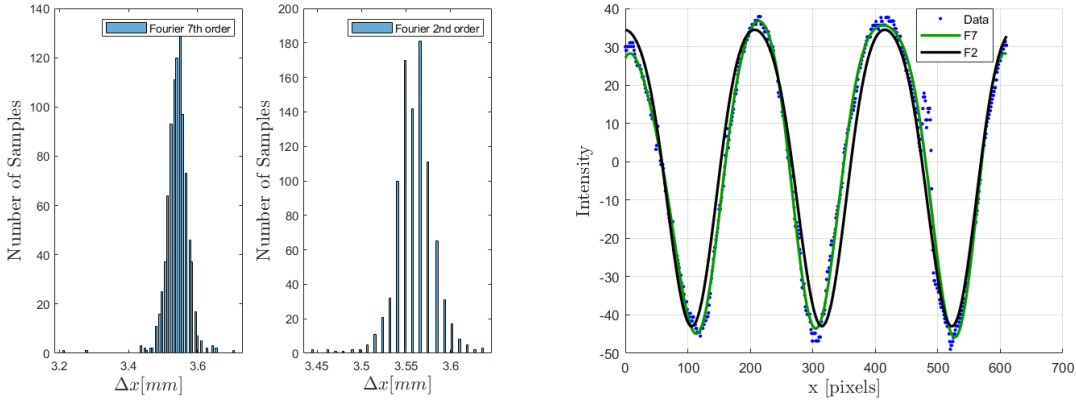


Figure 3 Histogram (left) and Fourier series fit (right) for the 7th and 2nd order Fourier series corresponding to the interrogation region for Case B, $X = 0.007$ m.

The fringe spacing was then used to calculate to the skin friction via equation (1):

$$C_f = \frac{2n\cos(\theta)\Delta x}{\lambda \int_0^{t_{run}} \frac{q_\infty(t)}{\mu(t)} dt} \quad (1)$$

where n is the index of refraction of the silicon oil, θ is the incident and reflected angle of the reflected light (the angle of the camera with respect to the local wall-normal), Δx is the measured fringe spacing, λ is the wavelength of the light source used, $q_\infty(t)$ is the freestream dynamic pressure as a function of time, $\mu(t)$ is the dynamic viscosity of the silicone oil as a function of time, and t_{run} is the total run time of the wind tunnel. Since accurate knowledge of the viscosity of the oil is critical, the viscosity of the oil was determined as a function of temperature utilizing the curve fit provided by Clearco (See Appendix 1) and is rewritten below in a modified form to change to dynamic viscosity.

$$\mu(T, \nu_0) = \rho 10^{(-6 + (\frac{763.1}{273+T} - 2.559 + \log(\nu_0)))} \quad (2)$$

Here μ is the dynamic viscosity (Pa·s), ρ is the density ($\frac{kg}{m^3}$), T is the temperature (°C), and ν_0 is the kinematic viscosity (cSt) at 25 °C all of which are properties of the silicone oil. Figure 4 shows the variation in kinematic viscosity, dynamic pressure, and temperature as functions of time for the wind tunnel run of the example just discussed.

Three streamwise locations were selected to take skin friction measurements, $X = -0.678$ m, $X = 0.007$ m, and $X = 0.907$ m. These locations were chosen since they all occur on the flat plate regions with no surface curvature and they represent the turbulent boundary layer initial condition, condition at the start of the ramp, and the condition at the end of the ramp, respectively. These measurements were repeated for each benchmark flow separation case and are reported in Table 1 below.

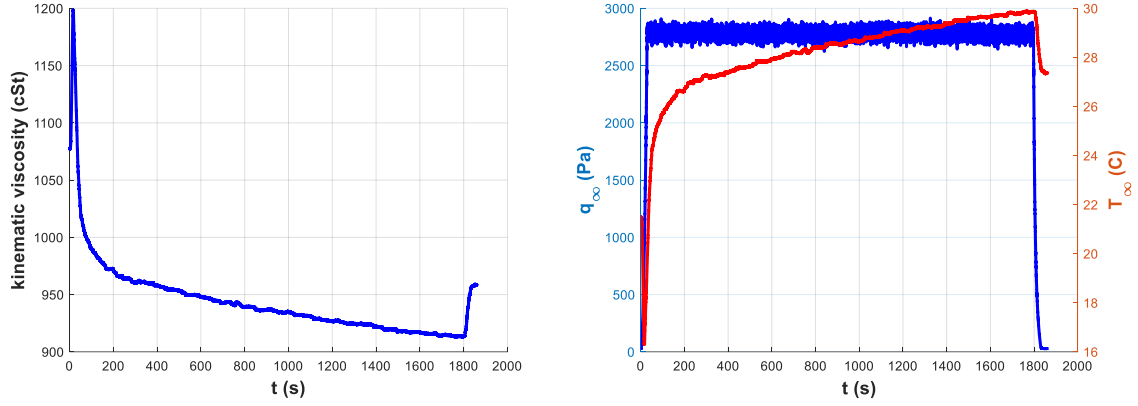


Figure 4 Kinematic viscosity, dynamic pressure, and temperature as functions time for example from Case B, $X = 0.007$ m, with the tunnel run time of 30 minutes.

Table 1 Skin friction coefficient values and uncertainties for each separation case. All measurements were taken near the centerline of the wind tunnel in the uniform flow region.

	X = -0.678 [m]	X = 0.007 [m]	X = 0.907 [m]
Case A	0.00235 ± 0.00016	0.00268 ± 0.00019	0.00019 ± 0.00002
Case B	0.00229 ± 0.00017	0.00272 ± 0.00020	0.00055 ± 0.00005
Case C	0.00211 ± 0.00017	0.00241 ± 0.00020	0.00084 ± 0.00007

Uncertainty Analysis

This section will outline the procedure used to calculate the uncertainty for the oil-film interferometry measurements reported. The uncertainty of C_f is a combination, via propagation, of the uncertainties of each of the parameters of C_f . The functional dependence of C_f is as follows:

$$C_f = f(\theta, \lambda, \Delta x, n, q_\infty(t), \mu(v_0, T(t))) \quad (3)$$

The sensitivities of C_f with respect to each of these dependent values were obtained by partial differentiation of equation (1). For ease of calculation, the integral in the denominator of equation (1) is defined as:

$$I = \int_0^{t_{run}} \frac{q_\infty(t)}{\mu(v_0, T(t))} dt \quad (4)$$

The uncertainty of C_f can then be written as:

$$u_{C_f} = \left[\left(\frac{\partial C_f}{\partial \theta} u_\theta \right)^2 + \left(\frac{\partial C_f}{\partial n} u_n \right)^2 + \left(\frac{\partial C_f}{\partial \Delta x} u_{\Delta x} \right)^2 + \left(\frac{\partial C_f}{\partial I} \frac{\partial I}{\partial q_\infty} u_{q_\infty} \right)^2 + \left(\frac{\partial C_f}{\partial I} \frac{\partial I}{\partial \mu} \frac{\partial \mu}{\partial v_0} u_{v_0} \right)^2 + \dots \left(\frac{\partial C_f}{\partial I} \frac{\partial I}{\partial \mu} \frac{\partial \mu}{\partial T} u_T \right)^2 \right]^{\frac{1}{2}} \quad (5)$$

The estimated uncertainties of each of the parameters in equation (5) is given below in Table 2. It should be pointed out that approximately 85% of the uncertainty of C_f is due to the

uncertainty associated with the variation in the viscosity. This includes both the 5% manufacturer's reported uncertainty as well as its variation with temperature and the uncertainty therein. The uncertainty in C_f of each of the measurements is shown in Table 1 and is approximately 5-9% of the local reported nominal value.

Table 2 Oil-film interferometry parameter uncertainty sources and estimates of their values.

Uncertainty Source	Estimated Uncertainty	Remarks
Incident angle: u_θ	± 0.051 (2.9°)	Primarily due to the geometry imposed small camera focal distance and the streamwise length of the interferogram region.
Fringe spacing: $u_{\Delta x}$	$\pm \Delta x_1 - \Delta x_2 $	Taken as the magnitude of the difference between Fourier series fit results. This dominates the random uncertainty.
Oil viscosity: u_{ν_0}	$\pm 5\%$ of ν_0	Manufacturer's specification. Uncertainty could be reduced by viscometer calibration.
Temperature: u_T	± 2 °C	Estimated based off standard k-type thermocouple uncertainty.
Dynamic pressure: u_{q_∞}	$\pm 0.3\%$ of FS	Full-scale range is 10 in H ₂ O. This value was doubled to account for the calibration uncertainty which is of approximately equal magnitude.
Oil index of refraction: u_n	± 0.002	Manufacturer's specification.
Light wavelength: u_λ	Negligible	The two wavelengths from the sodium lamp 589 nm and 589.6 nm are so close together the uncertainty is very small.

Appendix



Phone: 001 215 366-7860

Email: info@clearcoproducts.com

Viscosity to Temperature Chart Clearco Pure Silicone Fluids

